International Journal of Heat and Mass Transfer 76 (2014) 337–349

Contents lists available at ScienceDirect

International Journal of Heat and Mass Transfer

journal homepage: www.elsevier.com/locate/ijhmt

An experimental study of density ratio effects on the film cooling injection from discrete holes by using PIV and PSP techniques

Blake Johnson, Wei Tian, Kai Zhang, Hui Hu *

Department of Aerospace Engineering, Iowa State University, Ames, IA 50011-2271, United States

ARTICLE INFO

Article history:
Received 11 December 2013
Received in revised form 11 April 2014
Accepted 14 April 2014
Available online 21 May 2014

Keywords:
Film cooling of turbine blades
Cooling effectiveness quantification
Effects of coolant-to-mainstream density ratio
PIV measurements
PSP technique
Mass transfer analog

ABSTRACT

An experimental study was conducted to investigate the performance of film cooling injection from a row of circular holes spaced laterally across a flat test plate. While a high-resolution Particle Image Velocimetry (PIV) system was used to conduct detailed flow field measurements to quantify the dynamic mixing process between the coolant jet stream and the mainstream flows, Pressure Sensitive Paint (PSP) technique was used to map the corresponding adiabatic film cooling effectiveness on the surface of interest based on a mass-flux analog to traditional temperature-based cooling effectiveness measurements. The cooling effectiveness data of the present study were compared quantitatively against those derived directly from the temperature-based measurements under the same or comparable test conditions in order to validate the reliability of the PSP technique. The effects of the coolant-to-mainstream density ratio (*DR*) on the film cooling effectiveness were investigated by performing experiments at fixed blowing ratios by using either Nitrogen (*DR* = 0.97) or CO_2 (*DR* = 1.53) as the coolant streams for the PSP measurements. An accompanying analysis of scaling quantities, such as the coolant-to-mainstream momentum flux ratio, *I*, and bulk coolant-to-mainstream velocity ratio, *VR*, in addition to the most-commonly used blowing ratio (i.e., the coolant-to-mainstream mass flux ratio), *M*, was also conducted to illuminate the extent to which the flow scenario can be described using purely kinematic or dynamic means. It was found that the scaling quantities that give more weight to density ratio (i.e., blowing ratio, *M*, and then momentum ratio, *I*) have more success to collapse measurement data from varying density ratio of the coolant flows for the cases with relatively low coolant flow rates, while the coolant-to-mainstream bulk velocity ratio, *VR*, may be used with some success to scale the film cooling effectiveness for the cases with higher coolant flow rates.

1. Introduction

There is a great incentive to maximize the efficient operation of gas turbine engines for both economic and environmental reasons. As global transportation demands lean increasingly upon the use of such engines, large savings can be attained by even a marginal improvement in any of the systems that they rely on to function. Thermodynamic analysis reveals that thermal efficiency and power output of a gas turbine engine can be increased greatly with a higher turbine inlet temperature. Therefore, means to protect turbine components from high temperatures are necessary, typically through the implementation of film cooling techniques. While optimization of the film cooling of turbine blades possesses the potential for significant savings, a better understanding of the effects of a variety of controlling parameters on the coolant film behavior is necessary for such optimization.

Heat transfer experiments are traditionally used to assess the effectiveness of film cooling designs of turbine blades. Thermocouples were usually used to measure both fluid and surface temperatures in the earlier heat transfer experiments. However, since thermocouples can provide temperature measurements only at limited discrete points, it is very difficult to achieve temperature measurements (thereby, film cooling effectiveness) on the surface of interest with relatively high spatial and/or temporal resolutions. More recently, advanced optical-based thermometry techniques such as liquid crystal thermometry [1], infrared thermometry [2]; laser induced fluorescence [3] and temperature sensitive paint [4], which can achieve temperature distribution measurements on the surface of interest with much higher spatial and temporal resolutions in comparison with the thermocouple-based measurements, have been used in both transient and steady heat transfer experiments for turbine blade cooling studies. It should be noted

* Corresponding author. Tel.: +1 515 294 0094.
E-mail address: huhui@iastate.edu (H. Hu).

http://dx.doi.org/10.1016/j.ijheatmasstransfer.2014.04.028
0017-9310/

that, although useful information has been revealed from the heat transfer experiments with thermal-based measurements to examine the effectiveness of the film cooling designs of turbine blades, there always exists concerns and implications about the measurement uncertainties of the adiabatic temperature distributions on the surface of interest due to the effects of heat conduction through the test models in those heat transfer experiments.

Instead of conducting heat transfer experiments to measure the temperature distributions on the surface of interest, it is becoming increasingly popular to measure the film cooling effectiveness by conducting "cold" experiments with the Pressure Sensitive Paint (PSP) technique. Through a mass transfer analogy, the adiabatic film cooling effectiveness can be determined by measuring the distribution of oxygen concentration over the surface of interest by using the PSP technique with airflow as the mainstream flow and an oxygen-free foreign gas (e.g., nitrogen or CO_2 is used in the present study) as the coolant stream at an isothermal condition [4–12]. For example, Zhang and Jaiswal [5] used the PSP technique to measure the surface film cooling effectiveness on the surface of a turbine vane endwall. Ahn et al. [6] used the PSP technique to map the adiabatic film cooling effectiveness distributions near a gas turbine blade tip. The effects of the presence of a squealer, the locations of the film-cooling holes, and the tip-gap clearance on the film-cooling effectiveness were assessed in detail based on the quantitative PSP measurement results. Based on the PSP measurement results with a nitrogen stream as the coolant gas and airflow as the mainstream flow, Yang and Hu [7,8] investigated the effects of the blowing ratio and the existence of lands on the film cooling effectiveness of a turbine blade trailing-edge model. Similar approaches were also used by Rallabandi et al. [9] and Wright et al. [10,11] to study the film cooling effectiveness of the coolant streams injected from circular and shaped holes on flat plates. Dhungel et al. [12] used the PSP technique to assess the use of secondary cooling holes to counteract coolant jet vortex development, and found that the existence of the secondary cooling holes can greatly reduce the likelihood of the coolant jet to lift away from the protected surface. For the PSP measurements, since experimental studies were usually conducted at isothermal conditions, the measurement results are free from the heat conduction-related measurement errors that are frequently encountered in conventional heat transfer-based experiments for determining the adiabatic film cooling effectiveness.

So far, the blowing rate, which refers to the ratio of mass fluxes of the coolant jet stream to the mainstream flow and is expressed as $M = (\rho U)_c/(\rho U)_\infty$, is generally used to characterize the behavior of coolant jet flows and the resultant film cooling effectiveness over the surface of interest, where ρ indicates the fluid mass density, U indicates the bulk flow velocity, and the subscripts "c" and "∞" indicate the coolant jet and mainstream flows, respectively. By rewriting $M = DR * VR$, where DR is the density ratio of the coolant stream to the mainstream flows, and VR is the bulk velocity ratio of the coolant to mainstream flows, it is noted that, for a fixed blowing ratio M and mainstream flow conditions, an increase in density ratio, DR, requires a compensatory decrease in velocity ratio, $VR = U_c/U_\infty$. Similarly, the coolant-to-mainstream momentum flux ratio, $I = M^2/DR$, has also been used to characterize the behaviors of coolant jets in cross flows [10,13–15]. While extensive numerical and experimental studies have been conducted in recent years to investigate the characteristics of turbulent jets in cross flows pertinent to film cooling, very few studies can be found in literature that examine what are the proper scaling quantities/parameters to characterize the dynamic interaction and mixing between coolant jets and mainstream flows and the resultant cooling effectiveness over the surface of interest. With this need in mind, an explorative study was conducted in the present study to assess the applicability of the scaling quantities, which includes the most-commonly-used blowing ratio (i.e., coolant-to-mainstream mass flux ratio), M, the coolant-to-mainstream momentum flux ratio, I, and bulk velocity ratio, VR, in characterizing the behavior of the coolant jet flows and the resultant film cooling effectiveness over the surface of interest in order to shed some light on the underlying physics to discern the extent to which the dynamic interaction and mixing of the coolant jet and mainstream flows occur primarily due to the kinematics of the fluid flows or due to dynamic process that depend on the density disparity between the coolant stream and mainstream flows.

In the present study, an experimental investigation was conducted to assess the performance of film cooling injection from a row of circular holes spaced laterally across a flat test plate. In addition to using a high-resolution Particle Image Velocity (PIV) system to achieve detailed flow field measurements to quantify the dynamic interaction and mixing processes between the coolant jet stream and the mainstream flows, the Pressure Sensitive Paint (PSP) technique was used to map the corresponding adiabatic cooling effectiveness distributions on the surface of interest based on a mass transfer analog to traditional thermal-based film cooling effectiveness measurements. The cooling effectiveness data of the present study were compared quantitatively against those derived directly from the temperature-based measurements under the same or comparable test conditions in order to validate the reliability of the PSP technique as an effective experimental tool for turbine blade film cooling studies. To the best knowledge of the authors, this is the first effort of its nature. The effects of the density ratio between the coolant jet stream and mainstream flows, DR, on the behavior of the coolant jet flows as well as the resultant film cooling effectiveness distributions over the surface of interest were assessed by performing "cold" experiments at isothermal conditions with fixed blowing ratios (i.e., coolant-to-mainstream mass flux ratios) by using N_2 ($DR = 0.97$), air ($DR = 1.00$), and CO_2 ($DR = 1.53$) for the coolant streams. An accompanying analysis of the scaling quantities, such as the blowing ratio M, momentum flux ratio, I, and bulk coolant-to-mainstream velocity ratio, VR, was also performed. The detailed PIV flow field measurements were correlated with the adiabatic cooling effectiveness maps to elucidate underlying physics in order to explore/optimize design paradigms for improved cooling effectiveness to protect the critical portions of turbine blades from harsh environments.

2. The test model and experimental setup

2.1. The test model

The experimental study was conducted in a small open-circuit wind tunnel located at the Department of Aerospace Engineering of Iowa State University. The tunnel has a test section of 8.0 in. × 5.0 in. (i.e., 200 mm × 125 mm) in cross section. The walls of the test section are optically transparent. The tunnel has a contraction section upstream of the test section with honeycombs and screen structures installed ahead of the contraction section to provide uniform low-turbulence oncoming flow into the test section. The turbulence intensity at the inlet of the test section was found to be about 1.5%, as measured by using a hotwire anemometer.

Fig. 1 shows the schematic of the flat test plate used in the present study. The test model is made of a hard plastic material by using a rapid prototyping machine (i.e., 3D printer) that builds the model layer-by-layer with a resolution of about 25 μm. The upper surface of the test model was processed with fine sandpaper (i.e., up to 2000 grit) and specialty plastic polishes to achieve a very smooth, glossy finish. During the experiments, the test model was flush-mounted to the bottom wall of the wind tunnel test section, and a relatively large plenum (a cubic box of 152 mm in length,

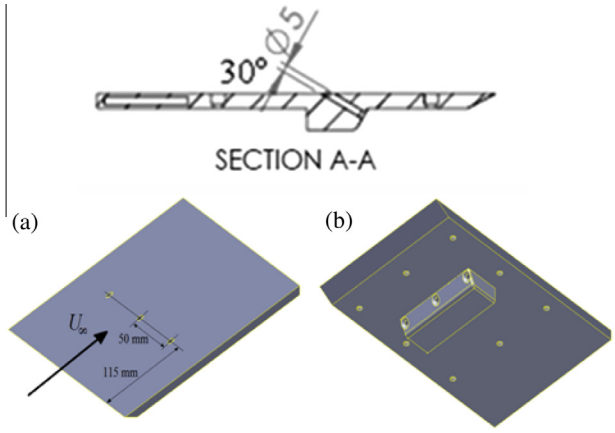

Fig. 1. The schematic of the test plate used in the present study. (a) Upper surface; circular holes with injection angle of 30°. (b) Lower surface: inlets are fluted to allow smooth entry of coolant stream into the injection holes.

width and height) was designed to settle the coolant flows (i.e., N_2, air and CO_2 for the present study). The plenum box was mounted underneath the test model via eight screws and sealed using a thin latex rubber gasket. The details of the plenum geometry and interior flow path within the plenum for the coolant stream can be found in Yang & Hu [7,8].

As shown in Fig. 1, the coolant stream was injected through a row of circular cylindrical holes of diameter D = 5.0 mm at an injection angle α = 30° relative to the upper surface of the flat test plate. The inlets of the coolant injection holes are fluted to allow smooth entry from the plenum and have a total axial length $L = 6D$, as measured from the outer entrance plane of the fluted inlets to the breakout plane at the upper surface of the test model. The axial centerlines of the coolant injection holes intersect the upper surface of the test model at a distance L = 115 mm from the leading edge of the test model. Thus, the boundary layer develops for a length of $22D$ before the mainstream flow encounters the coolant holes. In the present study, the main flow velocity at the inlet of the test section was fixed at U_∞ = 30 m/s, the corresponding Reynolds number is $Re = 2.2 \times 10^5$, based on the distance between the leading edge of the test plate and the coolant injection hole.

2.2. Flow field measurements using the PIV technique

In the present study, a high-resolution digital Particle Image Velocimetry (PIV) system was used to conduct detailed flow field measurements to quantify the dynamic interaction and mixing processes between the coolant and mainstream flows over of the test plate. Fig. 2 shows the schematic of the experimental setup used for the PIV measurements. During the experiments, the coolant jet stream and the mainstream airflow flows were seeded with ~1 μm oil droplets by using droplet generators. Illumination was provided by a double-pulsed Nd:YAG laser (NewWave Gemini 200) emitting two pulses of 200 mJ at the frequency-doubled wavelength of 532 nm with a repetition rate of 10 Hz. The laser beam was shaped to a sheet of sub-millimeter thickness by a series of mirrors, spherical, and cylindrical lenses. The laser sheet was aligned along the main stream flow direction bisecting the coolant hole in the middle of the test plate. A 14-bit high-resolution digital camera with a 2048 × 2048 pixel frame-straddling CCD camera (PCO2000) was used for the PIV acquisition with the axis of the camera perpendicular to the laser sheet. The CCD camera and the double-pulsed Nd:YAG lasers were connected to a workstation (host computer) via a Digital Delay Generator (Berkeley Nucleonics, Model 565), which controlled the timing of the laser illumination and the image acquisition.

After PIV image acquisition, instantaneous PIV velocity vectors were obtained by using a frame-to-frame cross-correlation technique involving successive frames of patterns of particle images in an interrogation window of 32 × 32 pixels, followed by two recursive passes of 16 × 16 pixels. An effective overlap of 50% of the interrogation windows was employed in PIV image processing. After the instantaneous velocity vectors (u_i, v_i) are determined, the vorticity (ω_z) can be derived. The distributions of the ensemble-averaged flow quantities such as the mean velocity, normalized Reynolds stress $(\overline{\tau} = -\overline{u'v'}/U_\infty^2)$ and turbulence kinetic energy $(T.K.E. = 0.5 * (\overline{u'^2} + \overline{v'^2})/U_\infty^2)$ were obtained from a cinema sequence of about 1000 or more frames of the instantaneous PIV measurements. The measurement uncertainty level for the velocity vectors is estimated to be within 2.0%, while the uncertainties for the measurements of ensemble-averaged flow quantities such as Reynolds stress and turbulent kinetic energy distributions are about 5.0%.

2.3. Film cooling effectiveness measurements by using the PSP technique

Adiabatic cooling effectiveness η_{aw} from a film cooling element is traditionally defined based on temperature measurements, and is expressed as:

$$\eta_{aw} = \frac{T_\infty - T_{aw}}{T_\infty - T_c}, \tag{1}$$

where T_∞ is the temperature of the main stream; T_{aw} is the adiabatic temperature of the surface of interest, and T_c is the temperature of the coolant stream. As described above, the primary challenge associated with the temperature-based method is in measuring the true adiabatic wall temperature despite the physical reality of heat conduction within the test model.

In the present study, rather than conducting temperature measurements on the surface of interest, the film cooling effectiveness was measured by using the PSP technique through use of a mass transfer analog [4–11]. Since PSP measurements are conducted by performing "cold" experiments at isothermal conditions, they eliminate the concerns and implications due to effects of heat conduction through the test models on the adiabatic wall temperature measurements over the surface of interest.

For PSP measurements, the surface of interest is coated with an oxygen-sensitive paint layer. Since the photoluminescence emission of PSP molecules is sensitive to O_2 — in that the presence of O_2 serves to reduce, or "quench", photoluminescence emission intensity of the excited PSP molecules — it can be used to measure the relative concentration of O_2 against the surface of interest. By preventing the oxygen molecules from the mainstream flow (i.e., airflow) from reaching the surface of interest via injection of O_2-free foreign gas through the coolant holes, the film cooling effectiveness distribution is determined in terms of the oxygen concentration distribution over the protected surface. Based on the mass transfer analogy and using the concentrations of oxygen rather than the temperature in Eq. (1), the adiabatic film cooling effectiveness can be expressed as:

$$\eta_{aw} = \frac{(C_{O_2})_{main} - (C_{O_2})_{mix}}{(C_{O_2})_{main} - (C_{O_2})_{coolant}} = \frac{(P_{O_2})_{air} - (P_{O_2})_{mix}}{(P_{O_2})_{air}}, \tag{2}$$

where $(C_{O_2})_{coolant}$ is zero for choice of an O_2-free coolant gas; thus, the above expressions can be expressed equivalently as some ratio subtracted from unity. Now, a potential pitfall arises in that the ratios $(C_{O_2})_{mix}/(C_{O_2})_{main}$ and $P(O_2)_{mix}/P(O_2)_{air}$ are not necessarily identical due to the differing molecular masses of the coolant gas and the mainstream flows. As described in Jones [16] and Charbonnier et al. [17], for the choice of a coolant gas whose molecular mass

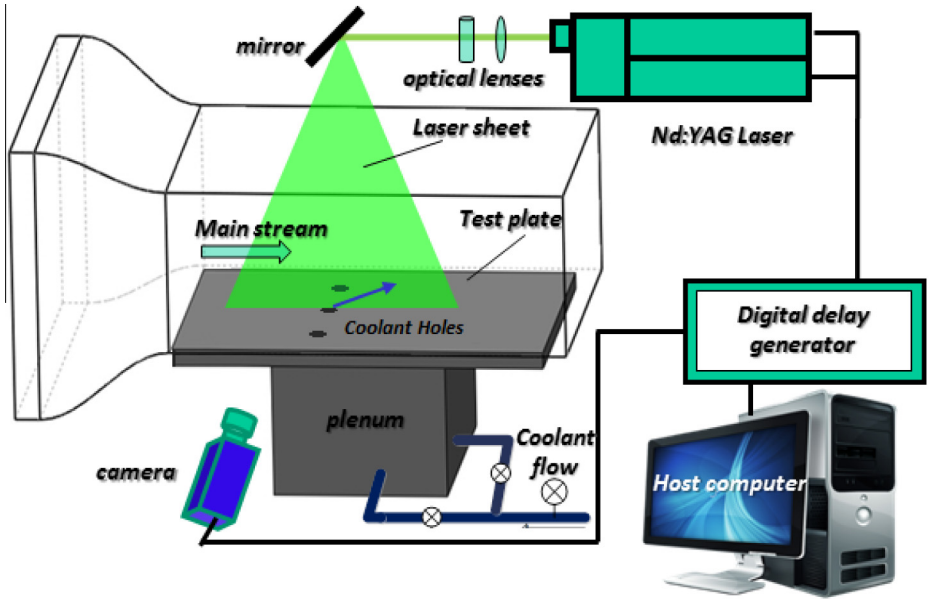

Fig. 2. Schematic of the experimental setup used for PIV measurements.

differs significantly from that of the mainstream, the cooling effectiveness as determined via measurement of the partial pressure of oxygen should be appropriately expressed as:

$$\eta = 1 - \frac{1}{\left[\left(\frac{(P_{O_2})_{air}}{(P_{O_2})_{mix}}\right)_{wall} - 1\right]\frac{M_{coolant}}{M_{air}} + 1}, \tag{3}$$

where $M_{coolant}$ and M_{air} are the molecular masses of the coolant gas and the mainstream air, respectively. Thus, if the coolant gas has similar density to air, such as Nitrogen (DR = 0.97), Eq. (2) will provide a reasonable approximation for the film cooling effectiveness. However, in a typical gas turbine engine the density ratio is significantly greater than unity. For this reason, the use of a foreign gas that has a greater density than air is sensible for the experimental study of film cooling effectiveness. In the present study, most of the experiments were performed by using CO_2 as the coolant gas (*i.e.*, DR = 1.53), with some cases using nitrogen (i.e., DR = 0.97) to investigate the effects of density ratio on the film cooling effectiveness.

As described above, since the photoluminescence intensity of the excited PSP molecules is a function of the concentration of oxygen molecules (i.e., partial pressure of oxygen), the quantitative information about the distributions of the oxygen concentration over the surface of interest can be obtained from an intensity ratio along with a PSP calibration curve. The oxygen concentration information can be directly converted into static pressure distributions for the case with air flow as the coolant stream. Intensity ratios for air and air-coolant mixture can be expressed as Eq. (4) respectively:

$$\frac{I_{ref} - I_b}{I - I_b} = f\left(\frac{P}{P_{ref}}\right), \tag{4}$$

where the reference intensity I_{ref} (with illumination, no flow, surrounding pressure uniform at 1.0 atm) is required in order to determine the intensity ratio, and background image intensity, I_b (no illumination and no flow) is used to remove the effects of camera noise, ambient illumination, and dark current. With a PSP calibration curve, the partial pressure of oxygen (i.e., oxygen concentration) on the surface of interest with both air and a foreign gas (i.e., CO_2 or N_2 for the present study) as the coolant stream can be calculated.

The above relation is inverted to give the necessary pressure fields to calculate cooling effectiveness η using Eq. (3) through the following relations:

$$\frac{(P_{O_2})_{air}}{(P_{O_2})_{ref}} = f^{-1}\left(\frac{I_{ref} - I_b}{I_{air} - I_b}\right), \tag{5}$$

and

$$\frac{(P_{O_2})_{mix}}{(P_{O_2})_{ref}} = f^{-1}\left(\frac{I_{ref} - I_b}{I_{mix} - I_b}\right). \tag{6}$$

Fig. 3 depicts the schematic of the experimental setup used in the present study to determine the PSP calibration curve. A test plate, which was painted with PSP molecules, was mounted in an enclosed test cell. The paint that was chosen for this experimental campaign is ISSI UniFIB due to its low temperature sensitivity (~0.5%/°C). The paint has peak emission intensity at 650 nm upon illumination with 390 nm UV light. A high-resolution CCD camera (i.e., 14-bit and 2048 pixels × 2048 pixels) fitted with a long-pass filter with a 610 nm cutoff wavelength was used for the PSP image acquisition. A constant temperature thermal bath system was used to control the temperature of the test plate mounted inside the test cell, which was monitored by using a K-type thermocouple with a measurement resolution of 0.1 °C. During the calibration experiment, a vacuum pump was employed to depressurize the test cell, and the pressure within the test cell was measured with a digital pressure transducer (i.e., DSA 3217 Module, Scanivalve Corp). A reference pressure of 1.0 atm (absolute) was used in the present study, which corresponds in the wind tunnel experiments to a condition of η = 0. Since it is feasible that some effectiveness experiments might indicate a possible maximum of η = 1.0, corresponding to a true zero absolute O_2 pressure, it was deemed necessary to calibrate for this condition rather than rely upon calibration curve extrapolation. For this data point the cell was flushed with pure CO_2 until the PSP emission reached a steady value.

In the present study, the calibration procedure was performed for a range of temperatures from 23.0 °C to 32.6 °C. For each temperature condition, all calibration points including the reference pressure were performed within the thermocouple resolution of a constant temperature. For example, all calibration data taken at 28.0 °C were likewise normalized by reference conditions of

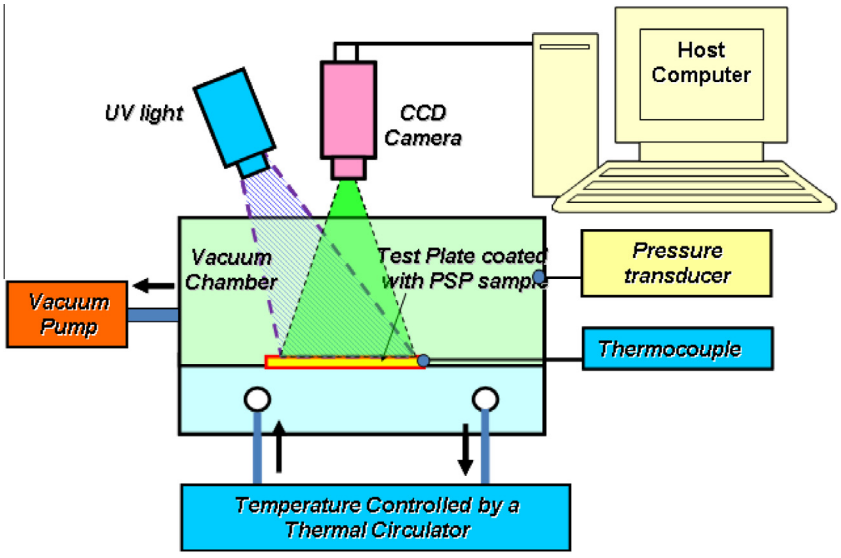

Fig. 3. Experimental setup for PSP calibration procedure.

28.0 °C as well, and so on for the other temperature conditions. Fig. 4 shows the normalized PSP calibration curves at different temperature levels. It is interesting to note that, while it is well known that the absolute value of the emission intensity of the excited PSP molecules are temperature dependent, the PSP calibration curves obtained at different temperature levels could be collapsed into a single curve by using an appropriate normalization method. A similar feature of the PSP calibration curves was also found by Liu et al. [18].

For the PSP image processing, in order to reduce the effects of camera noise on the measurement results, spatial averaging was performed in the present study on square interrogation windows of 9×9 pixels with 50% overlap to ensure complete sampling of the measurement data. The acquired PSP images typically have a magnification of about 0.093 mm/pixel, which results in a spatial resolution of 0.37 mm or 0.074D for the PSP measurement results. The measurement uncertainty for the film cooling effectiveness results given in the present study was estimated to be about ±0.04.

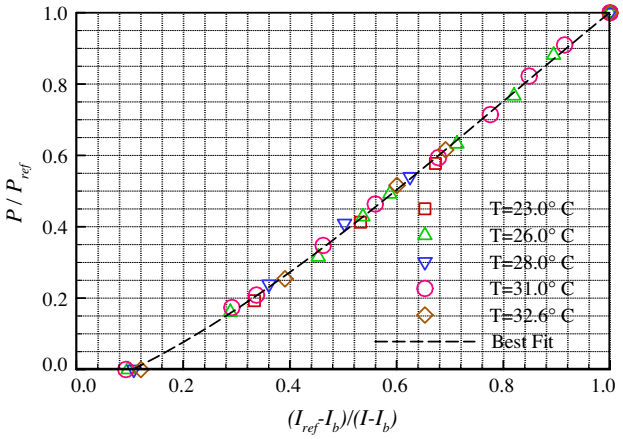

Fig. 4. The calibration curves for PSP measurements.

3. Measurement results and discussions

3.1. Flow characteristics of the oncoming boundary layer flow over the test plate

In the present study, the characteristics of the oncoming boundary layer of the mainstream flow over the test plate under different test conditions were measured by using the high-resolution PIV system. Fig. 5 shows some typical PIV measurement results in terms of the time-averaged flow field distribution over the test plate near the coolant injection hole in the middle of the test plate along with the transverse velocity profiles at several upstream locations relative to the coolant injection hole. From the measurement results given in Fig. 5, it can be seen clearly that, for the test case without coolant injection (i.e., $M = 0$ case), the velocity profile in the boundary layer of the oncoming mainstream flow was found to follow a 1/7th power law well at the leading edge of the coolant injection hole (i.e., at upstream location of $x/D = -1.0$). The thickness of the boundary layer, δ_{99}, at this location was found to be about 0.98D (i.e., $\delta_{99} \approx 0.98D$), while the displacement thickness of the boundary layer flow δ^* was found to be about 0.10D (i.e., $\delta^* \approx 0.10D$). Such characteristics in the boundary layer of the oncoming mainstream flow were found to match well with those of Baldauf et al. [19–21]. It can also be seen clearly that, for the test cases with non-zero coolant injection (i.e., the test cases with blowing ratio $M \neq 0.0$), there is a noted distortion in the velocity profiles of the oncoming flow at the same upstream locations of $x/D = -1.0$ and somewhat lesser distortion noted at the further upstream location of $x/D = -2.0$. As shown clearly in Fig. 5, the effect that increasing blowing ratio M has upon the oncoming mainstream flow is to thicken the boundary layer and reduce its streamwise momentum. Further upstream, i.e., at upstream locations of $x/D = -3.0$ and $x/D = -5.0$, there is little or no observable effect of the blowing ratio M upon the velocity profile of the oncoming mainstream flow.

While a number of experimental studies have been conducted in recent years using the PSP technique with mass transfer analogy to achieve quantitative film cooling effectiveness measurements, the PSP technique is still a fairly new technique to measure film cooling effectiveness in comparison to conventional temperature-based measurement methods. It is highly desirable and necessary to validate the reliability of the PSP-based measurements as an effective experimental tool for turbine blade film cooling studies. Surprisingly, very little can be found in literature to provide a quantitative comparison of the measured cooling effectiveness distributions by using the PSP technique against those derived

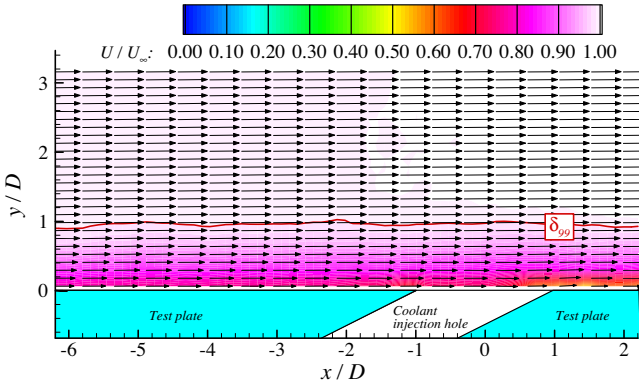

(a). Ensemble-averaged flow field for the test case with the blowing ratio of M=0.0

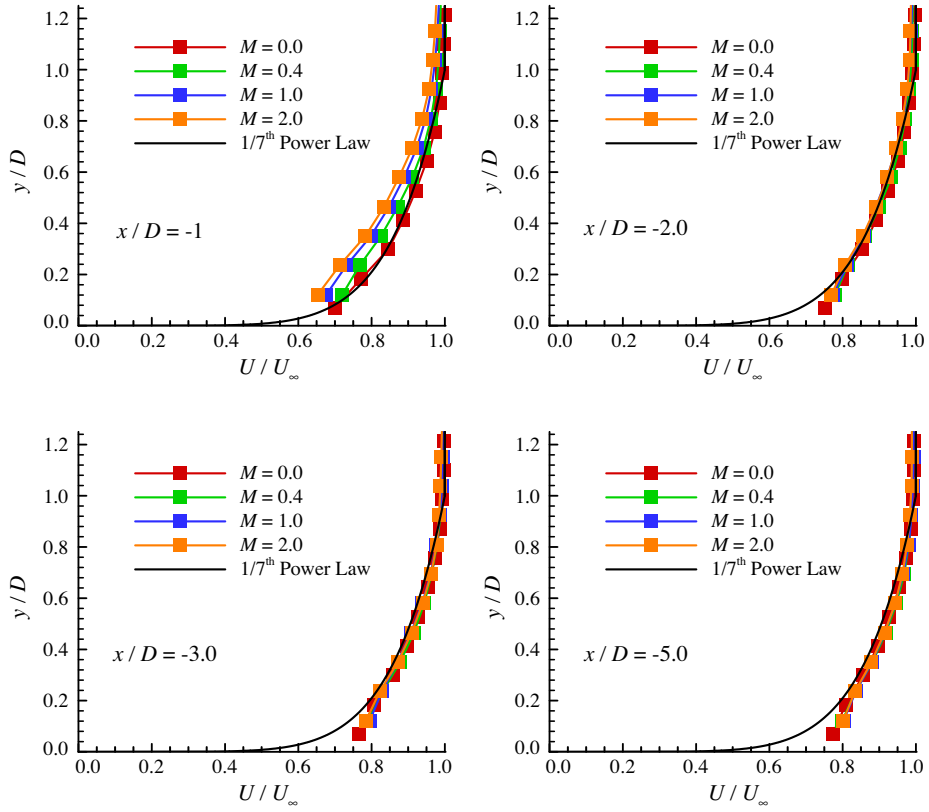

(b). The velocity profiles within the boundary layer upstream the coolant injection hole at the blowing ratio of M = 0.0, 0.4, 1.0, and 2.0, respectively.

Fig. 5. The flow characteristics of the oncoming mainstream flows over the test plate.

directly from the temperature-based measurements under the same or comparable test conditions. With this in mind, a comprehensive study was conducted in the present study to provide a quantitative comparison of the cooling effectiveness measurement results by using PSP technique with mass transfer analogy against those derived directly from temperature-based measurements for the same film cooling design under the same or comparable test conditions.

For the comparative study, a coolant stream of CO_2 (*i.e.*, DR = 1.53) was injected through circular holes with a blowing angle of 30° and a spanwise pitch of p/D = 3. Such geometry and experimental parameters were chosen due to an abundance of the temperature-based measurement data available in the published literature [19–24]. For example, by using a test model with almost the same geometry and experimental parameters as that used in the present study, Baldauf et al. [19–21] conducted a parametric study (i.e., by varying the blowing angle and the spanwise pitch between the coolant hole as well as the flow parameters such as blowing rate and density ratios) to quantify the adiabatic film cooling effectiveness on the surface of a test plate downstream a row of circular holes by measuring the surface temperature distributions over the test plate with an IR thermography system. Since the flow characteristics of the boundary layer of the oncoming flows for the present study were set to be almost identical as those of Baldauf et al. [19–21], the film cooling effectiveness over the test plate for the present study are expected to be the same or comparable as those of Baldauf et al. [19–21] under the same or comparable test conditions.

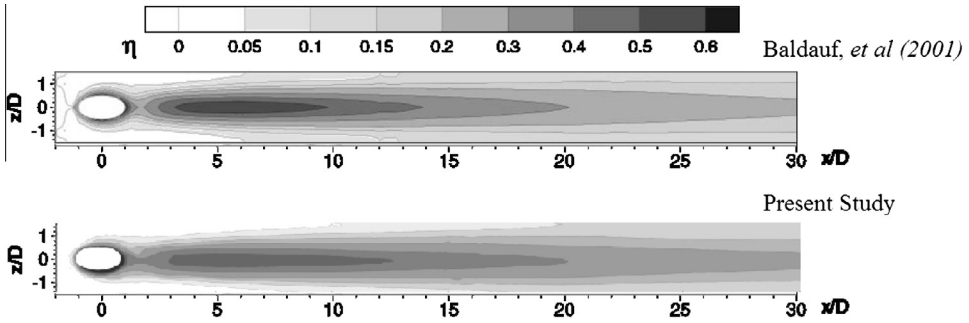

Fig. 6. Comparison of the measured cooling effectiveness distributions of the present study with that of Baldauf et al. [19,20] for the test case with the blowing ratio of $M = 0.85$ and density ratio of $DR \approx 1.5$.

Fig. 6 gives the measured film cooling effectiveness distribution downstream the circular coolant injection hole in the middle of the test plate at the blowing ratio of $M = 0.85$ and density ratio of $DR = 1.53$, i.e., CO_2 is used as the coolant stream for the PSP measurements in the present study. The measurement result of Baldauf et al. [20] under almost the same test conditions (i.e., same blowing ratio, same density ratio and very comparable oncoming boundary layer flow characteristics), but measured by using an IR thermometry system, was also given in Fig. 6 for the back-to-back comparison. It can be seen clearly that, the overall features revealed from the cooling effectiveness distributions obtained by using two different experimental techniques (PSP vs. IR thermometry) were found to be almost the same in a qualitative sense. It suggests that the measured film cooling effectiveness distribution of the present study with the PSP technique agrees well in general with that of Baldauf et al. [20] with the IR thermometry technique. However, some minor differences can also be identified based on the back-to-back comparison of the two measurement results. For example, for the region near peak cooling effectiveness from $3 < x/D < 10$, the measurement result of the present study seems to be slightly lower than those of Baldauf et al. [20]. The contours of the cooling effectiveness distribution for the present study were also found to be slightly "narrower" in the spanwise direction, in comparison with those of Baldauf et al. [20]. Such discrepancy is believed to be attributed to the fundamental differences between the two measurement techniques. As described above, since the PSP measurements of the present study were conducted under an isothermal condition to determine the film cooling effectiveness based on mass-transfer analog, it is free from the effects of heat conduction. However, the temperature-based measurement results reported in Baldauf et al. [20] were obtained by performing heat transfer experiments, which were very sensitive to the effects of the heat conduction through the test model. Therefore, it is within the realm of possibility that the results of Baldauf et al. [20] indicate a higher cooling effectiveness with a wider-spanning footprint due to the effects of heat conduction through the test model, particularly in the lateral direction. While measurement results of Baldauf et al. [20] are quoted to have a measurement uncertainty within 0.05, and the measurement uncertainty level of the present study was estimated to be about 0.04; a difference of up to 0.09 between the two measurements may, therefore, be considered within the statistical bounds of the agreement.

Following up the work of Baldauf et al. [19–21], the laterally-averaged cooling effectiveness data were also determined in the present study by averaging the cooling effectiveness data along the lateral direction over one full period of the hole spacing (i.e., in the region of $-p/2 < Z < p/2$) at each downstream location behind the coolant injection hole. Fig. 7 shows the profiles of the measured laterally-averaged cooling effectiveness of the present study with CO_2 as the coolant stream for the PSP measurements (i.e., the density ratio of $DR = 1.53$) as a function of the downstream distance from the exit of the coolant injection hole at the blowing ratio of $M = 0.5$ and $M = 1.0$. The temperature-based measurement results reported by Baldauf et al. [19,20] and other researchers [12,22–24] as well as the PSP measurement results of Rallabandi et al. [9] with the same or very comparable coolant hole configuration and test conditions as those of the present study were also given in the plots for a quantitative comparison. A summary of the experimental conditions of the compared studies is given in Table 1.

As shown clearly in Fig. 7(a), for the test case with relatively low blowing ratio of $M \approx 0.5$, density ratio of $DR \approx 1.5$ and coolant hole pitch of $p/D \approx 3.0$, the PSP measurement results of the present study lie very close to the temperature-based measurement results of Dhungel et al. [12], Kunze et al. [22] and Lutum and Johnson [23], especially through the region of $5 < x/D < 15$. The PSP measurement results of Rallabandi et al. [9] indicate somewhat lower cooling effectiveness but were measured at $M = 0.6$ and $DR = 0.97$; because of the higher blowing ratio and lower density ratio, it is reasonable to expect the coolant jet flow of Rallabandi et al. [9] would lift further away from the test surface than that of the present study, which would result in the reduced cooling effectiveness that they measured. It should be noted that three cases that used IR Thermography indicate higher effectiveness than the results of the present study, including Lawson and Thole [24], which were made at elevated mainstream turbulence intensities of Tu = 4.6% and 12.3%. Baldauf et al. [19,20] used very similar experimental conditions as those of the present study, including density ratio of $DR \approx 1.5$ and mainstream turbulence intensity level of Tu = 1.5%, and show cooling effectiveness levels slightly less than Lawson and Thole [24] for most of the streamwise fetch of their test plate.

Fig. 7(b) gives the measurement results for the test case with a relatively high blowing ratio of $M \approx 1.0$, density ratio of $DR \approx 1.5$, and coolant hole pitch of $p/D \approx 3.0$. The measurement results using PSP techniques (i.e., the data of the present study and those of Rallabandi et al. [9]) were found to lie very close to one another, especially for the region of $x/D > 6$. The cases measured using IR thermography show excellent agreement with one another and indicate higher effectiveness than those using PSP technique, with the exception of Kunze et al. [20], who used a larger hole pitch (i.e., $p/D = 4.0$ instead of $p/D = 3.0$) than the other cases. At this relatively high blowing rate of $M \approx 1.0$, the results of Baldauf et al. [19,20] show good agreement to those of the present study within the first five diameters and then overshoot it for the region of $x/D > 5$, though the results become similar once again near $x/D = 20$. Similar behavior is noted for Dhungel et al. [12] but with poorer agreement than Baldauf et al. [19,20] in the near field. It should be noted that the temperature-based measurements seem always to over-predict the cooling effectiveness slightly when compared to the PSP measurement data, especially in the regions

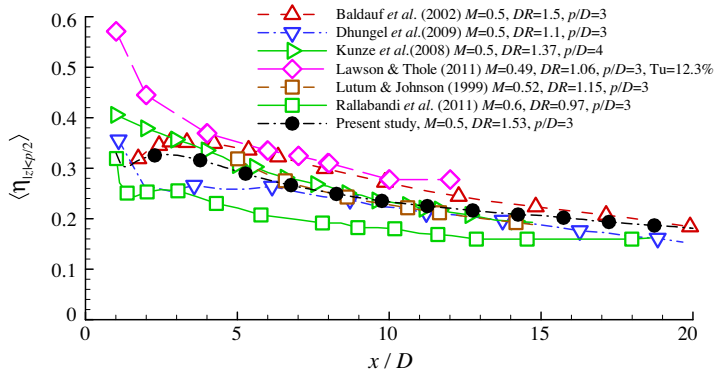

(a). The measurement results at blowing ratio of M≈0.50 and density ratio of DR≈1.5

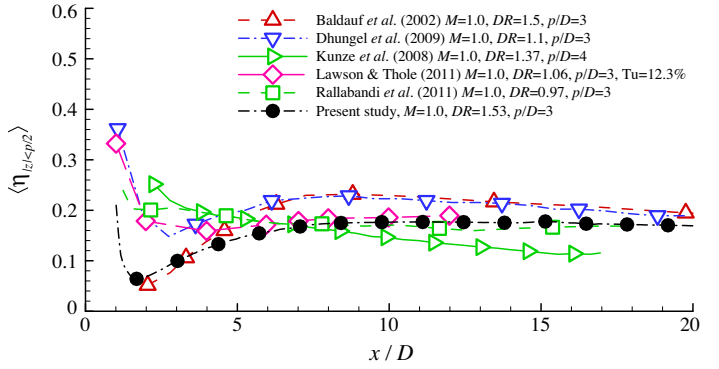

(b). The measurement results at blowing ratio of M≈1.00 and density ratio of DR≈1.5

Fig. 7. Comparison of laterally-averaged cooling effectiveness of the present study with the published results of previous studies at the same or comparable conditions.

Table 1
A summary of the experimental conditions of the compared studies.

Compared studies	M	P	I	V_r	p/D	Tu (%)	Measurement technique
Baldauf et al. [19,20]	0.50	1.50	0.17	0.33	3.0	1.5	IR thermography
	1.00	1.50	0.67	0.67	3.0	1.5	IR thermography
Dhungel et al. [12]	0.50	1.10	0.23	0.45	3.0	2	IR thermography
	1.00	1.10	0.91	0.91	3.0	2	IR thermography
Kunze et al. [22]	0.50	1.37	0.18	0.36	4.0	1.5	TSP
	1.00	1.37	0.73	0.73	4.0	1.5	TSP
Lawson and Thole [24]	0.49	1.06	0.23	0.46	3.0	12.3	IR thermography
	1.0	1.06	0.94	0.94	3.0	12.3	IR thermography
	0.49	1.06	0.23	0.46	3.0	4.6	IR thermography
Lutum and Johnson [23]	0.52	1.15	0.24	0.45	2.9	3.5	Thermochromic liquid crystals
Rallabandi et al. [9]	0.60	0.97	0.37	0.62	3.0	0.5	PSP
	1.00	0.97	1.03	1.03	3.0	0.5	PSP
The present study	0.50	1.53	0.16	0.33	3.0	1.5	PSP
	1.00	1.53	0.67	0.67	3.0	1.5	PSP

of peak cooling effectiveness (i.e., the regions with the lowest surface temperature on the test plate for the temperature-based measurements). It is conjectured that such over-prediction may be closely related to the effects of the heat conduction within the test models for the temperature-based measurements, as described above.

As aforementioned, the blowing rate, M, is widely used to characterize the behavior of coolant jet flows injected from the coolant holes and to evaluate the resultant film cooling effectiveness on the surfaces of interest for turbine blade film cooling studies. For fixed M and mainstream flow conditions, an increase in density ratio of the coolant stream, $DR = \rho_c/\rho_\infty$, would require a compensatory decrease in the velocity ratio of the two stream flows, $VR = U_c/U_\infty$. The effects of the density ratio, DR, on the behavior of coolant jet flow and the resultant cooling effectiveness over the surafce of interets were also exmined in the present study by using either nitrigen (DR = 0.97), air (DR = 1.00) or CO_2 (DR = 1.53) as the coolant stream for the PIV and PSP measurements, while the M was held constant during the experiments.

Fig. 8 show the PIV measurement results with either air (DR = 1.00) or CO_2 (DR = 1.53) as the coolant stream at the same blowing ratio of M = 0.85. As shown clearly from both the instantaneous and time-averaged PIV measurement results, the coolant stream out of the injection hole for both DR = 1.00 and DR = 1.53

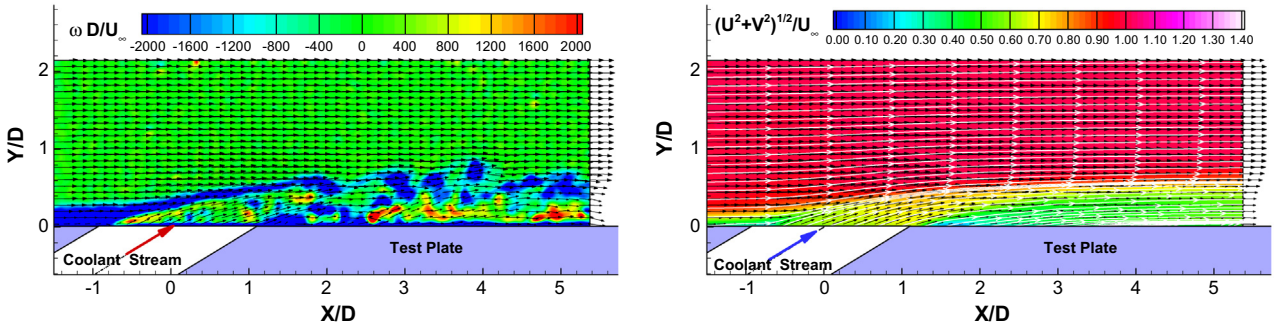

(a). Air as the coolant stream (*DR*=1.0)

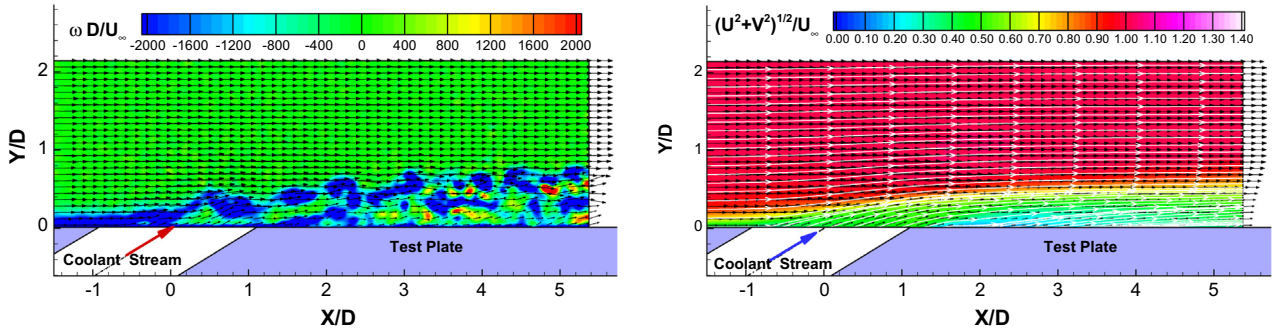

(b). CO_2 as the coolant stream (*DR*=1.53)

Fig. 8. Instantaneous and time-averaged PIV measurements results at the fixed blowing ratio of $M = 0.85$ with either air or CO_2 as the coolant jet stream.

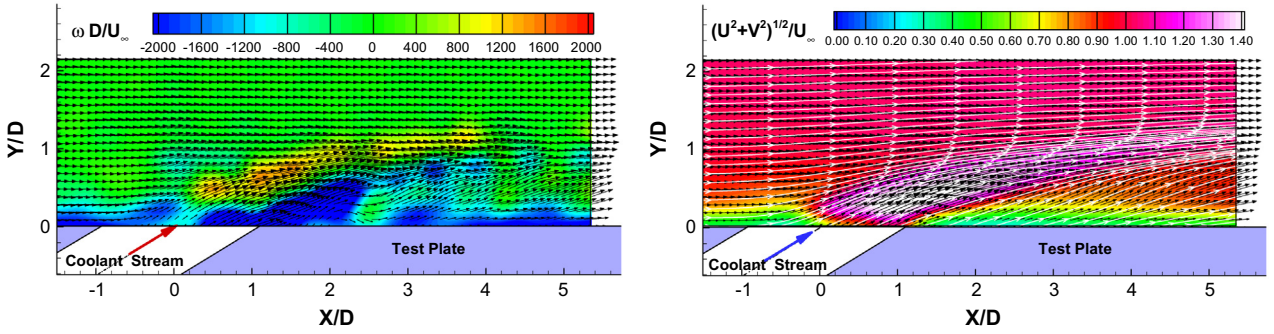

(a). Air as the coolant stream (*DR*=1.0)

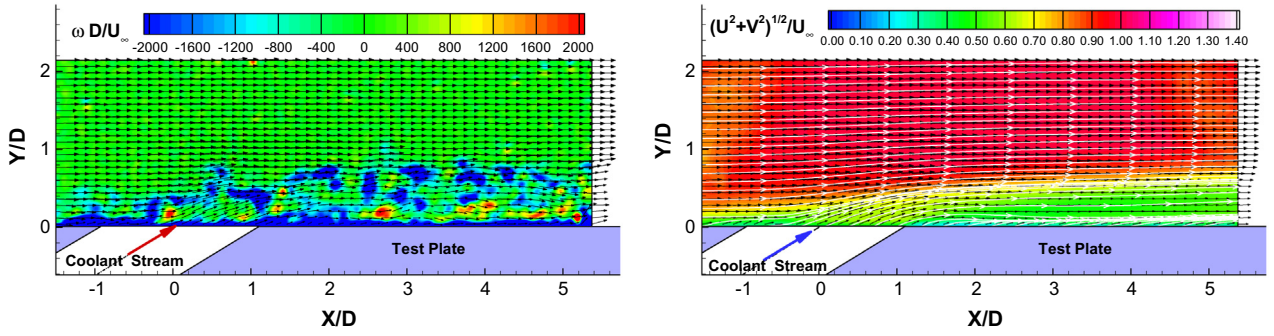

(b). CO_2 as the coolant stream (*DR*=1.53)

Fig. 9. Instantaneous and time-averaged PIV measurements results at the fixed blowing ratio of $M = 1.70$ with either air or CO_2 as the coolant jet stream.

cases were found to be able to stay attached to upper surface of the test plate to form a film over the test plate in the region downstream of the coolant injection hole at this blowing ratio. By carefully inspecting the flow features within the coolant sublayer, it can be seen that there is faster flow within the coolant sublayer for the cases with lower density ratio of $DR = 1.0$ (i.e., air or

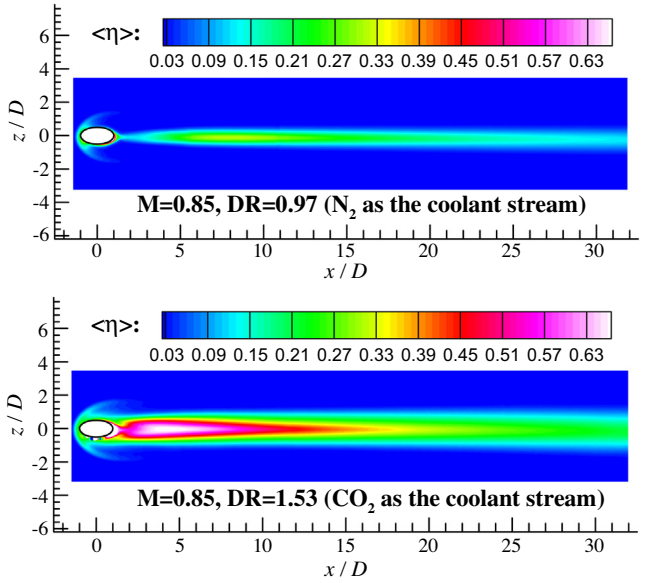

(a). Measurement results at blowing ratio of M=0.85

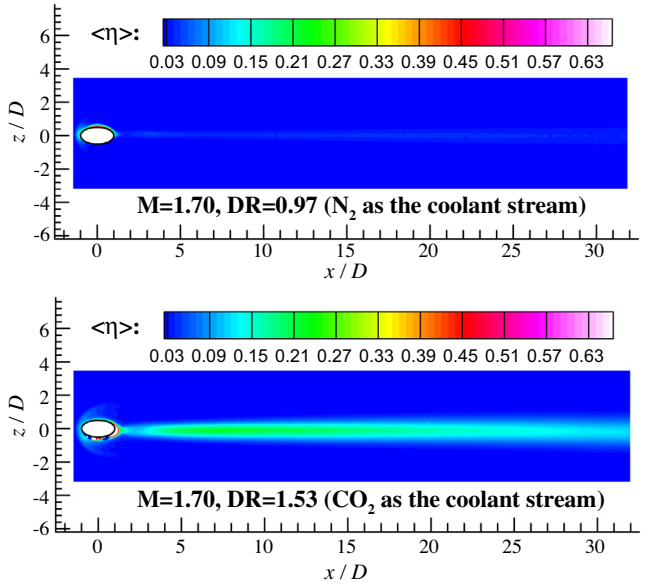

(b). Measurement results at blowing ratio of M=1.70

Fig. 10. Effects of the density ratio on the film cooling effectiveness (only the center hole is shown here).

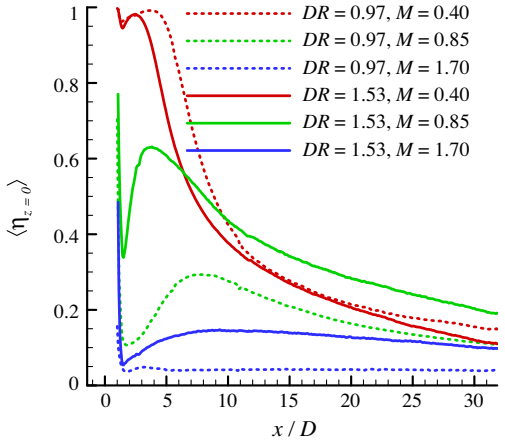

(a). Centerline cooling effectiveness profiles

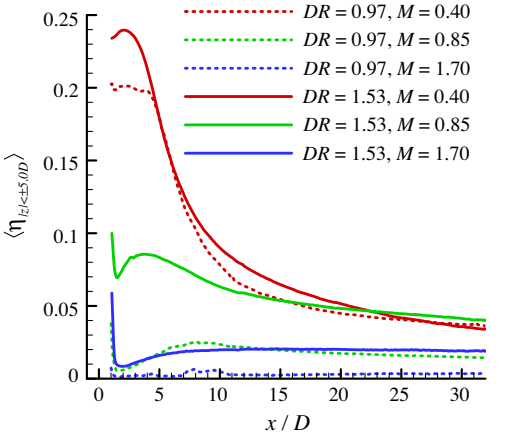

(b).Laterally-averaged cooling effectiveness profiles.

Fig. 11. Effects of the density ratio DR upon the film cooling effectiveness.

nitrogen as the coolant stream) than those with denser coolant flow (i.e., CO_2 as the coolant stream). The coolant jet stream with higher density ratio seems to be more concentrated within a thin film near the test plate and stays attached more firmly to the upper surface of the test plate. As a result, the film cooling performance over the test plate is expected to be much better for the case with higher density ratio (i.e., the case with CO_2 as the coolant stream), which was confirmed quantitatively from the PSP measurements given in Fig. 10.

Fig. 9 gives the PIV measurement results for the cases with a relatively high blowing ratio of M = 1.70. It can be seen clearly that the behavior of the coolant flow out of the injection hole is significantly different for the two compared cases even though the blowing ratio was matched. For the case with coolant stream of low density ratio (i.e., $DR \approx 1.0$), the coolant flow was found to lift off from the test plate and penetrate deeply into the mainstream. This behavior indicates that, at such relatively high blowing ratio of M = 1.70, the coolant jet flow with smaller density ratio would separate from the test plate, resulting in a poor film cooling performance over the surface of the test plate. However, for the case where the coolant stream had relatively high desnisty ratio (i.e., DR = 1.53), the coolant flow was remained attached, providing better film cooling to protect the upper surface of the test plate.

Fig. 10 gives the corresponding film cooling effectiveness maps on the test plate at M = 0.85 and M = 1.70. It can be seen clearly that the use of denser coolant stream (i.e., CO_2) would provide improved cooling effectiveness (i.e., much higher maximum cooling effectiveness values and much wider coolant coverage in the spanwise direction) than that of a less dense coolant stream (i.e., N_2) at the same blowing ratios. This result indicates that, at a fixed blowing ratio M, the coolant stream with a greater density ratio would provide better film cooling to protect the surface of interest than that with a lower density ratio. It should also be noted that, interestingly, evidence of reverse flow can be seen upstream of the coolant injection holes where finite effectiveness is measured in a halo-like feature that wraps around the coolant injection hole. Such a feature is most likely due to the presence of a horseshoe vortex that entrains some coolant from the jet stream, which is advected within the vortex around the coolant injection hole and then carried downstream, as described in [15,25,26]. A future paper will investigate the behavior of such a horseshoe vortex system as it pertains to the film cooling in greater detail.

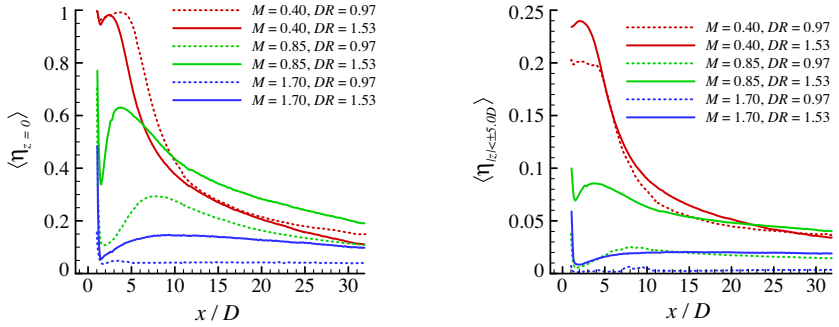

(a). The measurement results with matched blowing rate, M

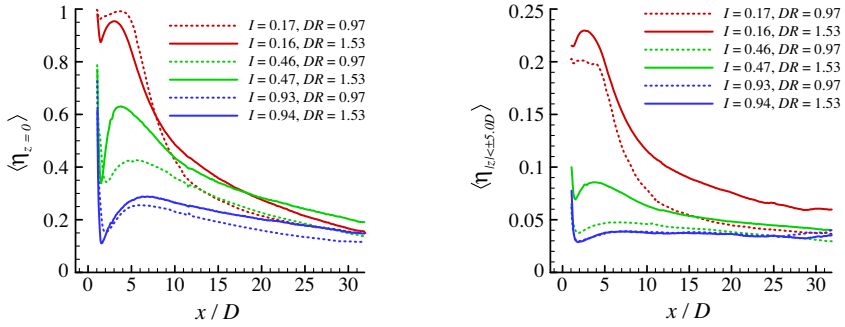

(b). The measurement results with matched momentum flux ratio, I

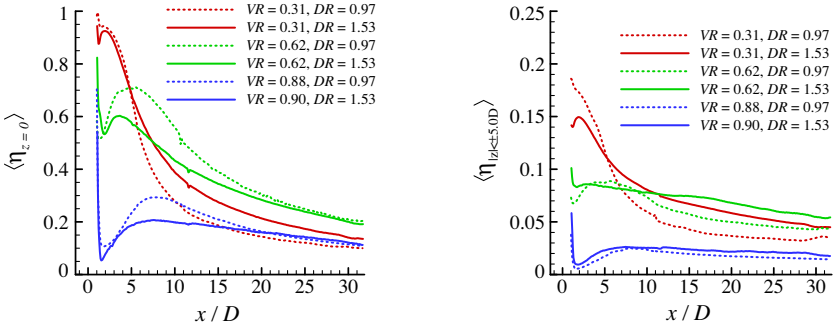

(c). The measurement results with matched velocity ratio, VR.

Fig. 12. The measured film cooling effectiveness along the centerline of the coolant injection holes and the laterally-averaged film cooling effectiveness with two different coolant gases: dashed lines represent N_2, solid lines represent CO_2.

Fig. 11 shows the profiles of the measured cooling effectiveness data along the centerline of the coolant injection hole and the laterally-averaged film cooling effectiveness as a function of the downstream distance away from the coolant injection hole at the fixed blowing ratio of $M = 0.40$ (low), 0.85 (medium) and 1.70 (high), which can be used to reveal the effects of the coolant-to-mainstream density ratio on the film cooling performance of the coolant jet streams over the surface of interest more clearly and quantitatively. It can be seen clearly that, concerning the physics of the film cooling, there is little difference between the coolant streams of different density for the cases with relatively low blowing ratios (i.e., for the cases of $M = 0.40$), suggesting that the coolant stream is able to remain well-attached to the test plate to protect the surface of interest at relatively small blowing ratio. However, as shown clearly from the PIV measurements given in Fig. 10, the coolant jet stream with lower density ratio tends to lift off much earlier and separate more easily from the test plate, compared with those of denser coolant stream, as the blowing ratio increases. As a result, the film cooling effectiveness over the surface of interest was found to become dependent upon the coolant-to-mainstream density ratio when the blowing ratio becomes relatively high. As shown quantitatively from the measurement results given in Fig. 11, the use of the coolant stream with higher density would result in increased cooling effectiveness over the surface of interest by the measures of both the centerline and laterally-averaged cooling effectiveness for the cases of $M = 0.85$ and 1.70.

The PIV and PSP measurement results given above reveal clearly that the blowing ratio, M, alone would not be able to successfully categorize the behavior of coolant jet stream as well as the resultant film cooling effectiveness on the surfaces of interest. In the present study, an explorative study was also conducted to assess the applicability of other scaling quantities such as the coolant-to-mainstream momentum flux ratio, $I = M^2/DR$, and bulk velocity ratio, $VR = U_c/U_\infty$, in comparison to the most-commonly used blowing ratio (i.e., coolant-to-mainstream mass flux ratio), M, in characterizing the film cooling effectiveness over the surface of interest in order to reveal the extent to which the flow scenario can be described by using purely kinematic or dynamic means. By conducting such analysis, it is hopeful to illuminate the underlying physics to discern the extent to which the interaction and mixing of the coolant jet and mainstream flows occur primarily

due to the kinematic conditions of the flow field or due to the dynamic processes that depend on the density disparity between the two streams.

With this in mind, a set of experiments were conducted to measure the film cooling effectiveness on the surface of interest at closely-matched values of the blowing ratio, *M*, momentum ratio, *I*, and velocity ratio, *VR*, with either N_2 ($DR = 0.97$) or CO_2 ($DR = 1.53$) as the coolant stream for the PSP measurements. The measured cooling effectiveness along the centerline of the coolant injection hole and the laterally-averaged film cooling effectiveness are given in Fig. 12(a)–(c), respectively. In this order, the successive subfigures represent decreasing weighting of the scaling by density ratio, *DR*, or, conversely, the order of increasing importance of flow kinematics upon the resultant film cooling effectiveness. In the plots, the red curves represent the slowest of the three quantities in each plot, blue curves are used for the highest, and green curves show the intermediate coolant flows. Interestingly, the red curves were found to be always little-affected by differences in density ratio for matched mass-flux ratio *M*, and momentum-flux ratio *I*, but significant far-field disparity is noted for the cases of velocity ratio-matching, which suggests that the influence of density ratio, *DR*, is important at low mass-flux ratio (i.e., blowing ratio), *M*, and momentum-flux ratio, *I*, and those quantities can successfully scale film cooling flows across differences in density (or temperature for thermal-based experiments, equivalently). However, the green and blue curves indicate that increases in density ratio, *DR*, result in poor matching of mass-flux ratio *M*, and momentum-flux ratio *I*, across the differences in the density ratio, *DR*, as the coolant injection increases. This trend is reversed for the *VR*-matching cases, for which the blue curves trend near each other for both density ratio values, but the red slow-coolant curves agree in the near-field but show disparity in the far-field, with the more-dense coolant stream resulting in better cooling effectiveness. The green curves trend closely to each other in the far-field but not in the near-field. Thus, it seems that, as the coolant flow increases, the velocity ratio, *VR*, becomes increasingly useful to describe the cooling effectiveness for the test cases with differing density ratios. It is worth mentioning here that the Richardson number of these flows, which represents the ratio between the buoyancy forces to the gravity forces for the flows, was found to be always very small, i.e., almost negligible, for all the cases investigated in the present study, which it indicates that buoyancy force is not a likely culprit for the tendency of the coolant gases with different densities to behave differently.

4. Summary and conclusions

An experimental study was conducted to quantify the performance of film cooling injection from a row of circular holes spaced laterally across a flat plate. While a high-resolution Particle Image Velocimetry (PIV) system was used to conduct detailed flow field measurements to quantitatively visualize the dynamic mixing process between the coolant jet stream and the mainstream flows, the Pressure Sensitive Paint (PSP) technique was used to achieve adiabatic film cooling effectiveness measurements based on a mass-flux analog to traditional temperature-based cooling effectiveness measurements. The cooling effectiveness data of the present study were compared quantitatively against those derived directly from the temperature-based measurements under the same or comparable test conditions to validate the reliability of the PSP measurements for turbine blade film cooling studies.

While the focus of the present study has been placed on the effects of the density differences of the coolant streams on the resultant cooling effectiveness on the surface of interest at fixed blowing ratios, the applicability of other scaling quantities such as the coolant-to-mainstream momentum flux ratio and the bulk velocity ratio, in addition to most-commonly-used blowing ratio (i.e., coolant-to-mainstream mass flux ratio), in characterizing the performance of film cooling over the surface of interest have also been explored. The PIV measurement results reveal clearly that the coolant jets out of the injection holes would be able to stay attached to the test plate to form film flows to protect the surface of interest at relatively low blowing ratios. However, as the blowing ratio increases, the coolant jets with lower coolant-to-mainstream density ratios tend to separate from the test plate easily, while the coolant jets with higher density ratios are likely to remain attached to the test plate at the same blowing ratios, offering improved film cooling performance to protect the surface of interest. As a result, there is a corresponding increase in the film cooling effectiveness for the coolant jet flows with elevated density ratios. For the cases where the coolant jet flows were found to separate from the test plate, the film cooling effectiveness over the test plate would become very low in spite of the injection of large amounts of coolant.

The analysis with different scaling quantities indicates that the quantities that give more weight to density ratio (i.e., coolant-to-mainstream mass flux or blowing ratio and momentum flux ratio) would be more successful to collapse measurement data from varying density of coolant jet streams for the cases with relatively low coolant flow rates, while the coolant-to-mainstream bulk velocity ratio may be used with some success to scale the film cooling effectiveness data for coolant jets of higher velocities. The intriguing nature by which such these quantities tend to have preferential success at scaling coolant jets of different flow rates begs deeper analysis. Additionally, some observations of film cooling effectiveness patterns reminiscent of the presence of a horseshoe vortex begs a deeper analysis into the effects that closer spacing of coolant holes might have upon the jet behavior, which will be performed in a future paper.

Conflict of interest

None declared.

Acknowledgments

The technical assistance of Drs. Jose Cordova, Wontae Hwang and Jonathon Slepski of GE Global Research Center and Mr. Bill Rickard and Mr. Marc Regan of Iowa State University are greatly appreciated.

References

[1] J.C. Han, S. Dutta, S. Ekkad, Gas Turbine Heat Transfer and Cooling Technology, Taylor and Francis, New York, 2000, pp. 540–559.
[2] C. Saumweber, A. Schulz, S. Witting, Free-Stream Turbulence Effects on Film-Cooling with Shaped Holes, J. Turbomach. 125 (1) (2003) 65–73.
[3] M.K. Chyu, Y.C. Hsing, Use of a thermographic fluorescence imaging system for simultaneous measurement of film cooling effectiveness and heat transfer coefficient, in: ASME Paper 96-GT-430, 1996.
[4] L.M. Wright, Z. Gao, T.A. VArvel, C.J. Han, Assessment of steady state psp, tsp, and ir measurement techniques for flat plate film cooling, in: Summer Heat Transfer Conference, San Francisco, ASME Paper HT2005-72363, 2005.
[5] L.J. Zhang, R.S. Jaiswal, Turbine nozzle endwall film cooling study using pressure-sensitive paint, J. Turbomach. 123 (4) (2001) 730–738.
[6] J. Ahn, S. Mhetras, J.C. Han, Film-cooling effectiveness on a gas turbine blade tip using pressure-sensitive paint, ASME J. Heat Transfer 127 (5) (2005) 521–530.
[7] Z. Yang, H. Hu, Study of trailing-edge cooling using pressure sensitive paint technique, J. Propul. Power 27 (3) (2011) 700–709.
[8] Z. Yang, H. Hu, An experimental investigation on the trailing edge cooling of turbine blades, Propul. Power Res. 1 (1) (2012) 36–47.
[9] A.P. Rallabandi, J. Grizzle, J.C. Han, Effect of upstream step on flat plate film-cooling effectiveness using PSP, J. Turbomach. 133 (2011) 041024-1–041024-8.
[10] L.M. Wright, S.T. McClain, M.D. Clemenson, Effect of density ratio on flat plate film cooling with shaped holes using PSP, J. Turbomach. 133 (2011) 041011-11.

[11] L.M. Wright, S.T. McClain, M.D. Clemenson, Effect of freestream turbulence intensity on film cooling jet structure and surface effectiveness using PIV and PSP, J. Turbomach. 133 (2011) 041023-12.
[12] A. Dhungel, Y. Lu, W. Phillips, S.V. Ekkad, J. Heidmann, Film cooling from a row of holes supplemented with anti-vortex holes, J. Turbomach. 131 (2009) 021007–021010.
[13] Y. Komotani, I. Greber, Experiments on a turbulent jet in a cross flow, AIAA J. 10 (11) (1972) 1425–1429.
[14] R.J. Goldstein, E.R.G. Eckert, F. Burggraf, Effect of hole geometry and density on three dimensional film cooling, Int. J. Heat Mass Transfer 17 (1974) 595–607.
[15] E.J. Gutmark, I.M. Ibrahim, S. Murugappan, Circular and noncircular subsonic jets in cross flow, Phys. Fluids 20 (2009) 075110.
[16] T.V. Jones, Theory for the use of foreign gas in simulating film cooling, Int. J. Heat Fluid Flow 20 (1999) 349–354.
[17] D. Charbonnier, P. Ott, M. Jonsson, F. Cottier, T.H Kobke, Experimental and numerical study of the thermal performance of a film cooled turbine platform, in: Proc. Of ASME Turbo Expo 2009: Power for Land, Sea and Air, June 8–12, 2009.
[18] L. Liu, S.F. Yang, J.C. Han, Influence of coolant density on turbine blade film-cooling with axial shaped holes, in: Proceedings of the ASME 2012 Summer Heat Transfer Conference, Rio Grande, Puerto Rico, July 8–12, 2012.
[19] S. Baldauf, A. Schulz, S. Wittig, High-resolution measurements of local heat transfer coefficients from discrete hole film cooling, J. Turbomach. 123 (2001) 749–757.
[20] S. Baldauf, A. Schulz, S. Wittig, High-resolution measurements of local effectiveness from discrete hole film cooling, J. Turbomach. 123 (2001) 758–765.
[21] S. Baldauf, M. Scheurlen, A. Schulz, S. Wittig, Correlation of film-cooling measurements from thermographic measurements at engine-like conditions, J. Turbomach. 124 (2002) 686–698.
[22] M. Kunze, S. Preibisch, K. Vogeler, K. Landis, A. Heselhaus, A new test rig for film cooling experiments on turbine endwalls, in: ASME IGTI Paper No. GT2008-51096, 2008.
[23] E. Lutum, B.V. Johnson, Influence of the hole length-to-diameter ratio on film cooling with cylindrical holes, J. Turbomach. 121 (2009) 209–216.
[24] S.A. Lawson, K.A. Thole, Effects of simulated particle deposition of film cooling, J. Turbomach. 133 (2011) 021009-1–021009-9.
[25] T.H. New, T.T. Lim, C.S. Luo, Elliptic jets in cross-flow, J. Fluid Mech. 494 (2003) 119–140.
[26] B. Johnson, K.T. Christensen, G.E. Elliott, Structural characteristics of a heated jet in cross-flow emanating from a raised, circular stack, Exp. Fluids 54 (2013) 1543.